A NOVEL TECHNIQUE TO SIMULATE THE PERIODIC BOUNDARY CONDITIONS IN MAXWELL'S EQUATIONS

K. Fu and P.-f. Hsu
Mechanical and Aerospace Engineering Department
Florida Institute of Technology, Melbourne, FL 32901, USA

BACKGROUND

Because structures can significantly change the radiative properties of surfaces, the application of periodic structures is of great interest in electrodynamics, optics, and thermal engineering. A good example is frequency-selective surface or wavelength-selective surface, which is typically built with layers of materials in periodic patterns, either in one or two dimensions.

As the number of periodic replicas grows, the simulation over the whole system becomes impractical. An intuitive solution is to model only one period of unit instead of the whole computation domain, and then apply periodic boundary condition (PBC) to simulate the periodic effect. However, there are fundamental difficulties in applying the periodic boundary condition in the time domain. Current techniques used to simulate periodic boundary conditions can be divided into two categories: field-transformation methods and direct field methods. These methods all have drawbacks.

PHASE DIFFERENCE AT THE PERIODIC BOUNDARIES

The following figure is presented to demonstrate scattering at the periodic boundary and test the new technique for PBC simulation. In this problem, the computation domain is topped and bottomed by two PML layers, and a planar source wave is projected towards a dielectric medium from the scattering field/total field interface. The whole system is enclosed by left and right periodic boundaries, with a distance l. The critical problem is to address the phase shift Φ from the left boundary to the right boundary. The phase shift $\Phi = -k_x l$, where $k_x = -k\sin\theta$ and $k = \omega/c$. θ is the incident angle, ω is the angular frequency, and c is the light speed in a vacuum. The corresponding time shift is $\zeta = \Phi/\omega$.

Figure 1(a) shows the general 3D space discretization used in Yee algorithm [3]. Figure 1(b) illustrates a periodic boundary condition simulation of a 2D transverse electric (TE) polarization case and nx denotes the number of grids in x-direction. If Δx is the grid size in x-direction, then period length $L = nx\cdot\Delta x = l+\Delta x/2$. In Fig. 1(b), the left and right solid lines denote the physical computation boundaries, while the dash lines stand for virtual boundaries which are needed to complete the time advance at the physical computation boundaries. The left virtual boundary is a period L away from the right physical boundary, as are the left physical boundary and right virtual boundary. As demonstrated in Fig. 1(b), only one field component is needed on each side, i.e., $H_y(nx, j)$ on the right physical boundary is needed to simulate the periodic component $H_y(0, j)$ on the left virtual boundary so that $E_z(1, j)$ on the left physical boundary can be updated at the next time step.

TIME DOMAIN TO FREQUENCY DOMAIN TRANSFORMATION

As mentioned above, the adaption of field component from one physical periodic boundary to its opposite virtual boundary is required to complete the simulation of PBC scattering (e.g., utilizing the information of $H_y(nx, j)$ at $H_y(0, j)$ and the information of $E_z(1, j)$ at $E_z(nx+1, j)$ as shown in Fig. 2(b)). The fundamental electromagnetics theorems indicate that electromagnetic energy propagates

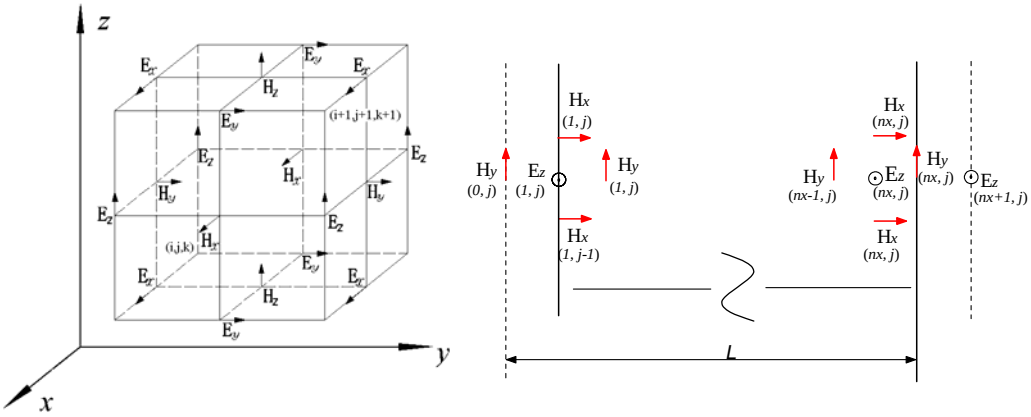

(a) Yee's FDTD grid. (b) 2D periodic boundary grid.

Figure 1. The FDTD grids at the interior and boundaries.

as a wave. For example, electric field has the form of $E_o e^{j(\omega t+\Phi)}$, i.e., a function of amplitude E_o and phase Φ. Thus, a phase shift of Φ can be handled easily by multiplying $e^{j\Phi}$, without the need to allocate memory for additional grids. Obviously the frequency domain methods have advantages over time domain methods in terms of computation load and grid mesh storage. However, the FDTD algorithms are time domain simulation: thus, the transformation between time domain and frequency domain is necessary.

Instantaneous Transformation Technique

A novel instantaneous transformation technique has been developed to solve the problem. The following phasor diagram illustrates the essence of this technique. As shown in Fig. 2, the vector *OA* stands for the known $\tilde{E}_{n-1}$ phasor field at time step *n*-1. The vector *OB* stands for the anticipated phasor field at next time step, and we have,

$$\tilde{E}_n^* = \tilde{E}_{n-1} e^{j\omega\Delta t} \tag{1}$$

According to the Yee algorithm, the real value of an electric field at time step *n* can be updated with the magnetic field at a prior half time step, *n*-1/2: and the update of the components lying inside a periodic boundary can be achieved by using the magnetic field on its neighboring virtual boundary – for example, in Fig. 1(b) the update of $E_z(1, j)$ can be realized with $H_y(0, j)$, which is equal to $\mathrm{Re}\{H_y(n, j)e^{-j\Phi}\}$. Thus, the computational real value of an electric field on the physical boundary at time step *n* is achieved, defined as E_n. As Fig. 2 shows, there is a difference between the real part of $\tilde{E}_n^*$ and E_n, and the difference is given by $\Delta = E_n - \mathrm{Re}\{\tilde{E}_n^*\}$. Thus, with the aid of Fig. 2, *O'C* is the phasor field at time step *n*, where *O'* is the new origin on the imaginary axis. Since $\omega\Delta t << 1$, the phasor field at the current time step can be written as

$$\tilde{E}_n = \tilde{E}_n^* + \Delta - j\cdot|O'O| = \tilde{E}_{n-1} e^{j\omega\Delta t} + \Delta - j\cdot\frac{\left|\tilde{E}_{n-1} e^{j\omega\Delta t} + \Delta\right|}{(\cos\alpha + \sin\alpha\cdot\cot\beta)}. \tag{2}$$

As previously mentioned, directly using the intercept of the perpendicular bisector may result in stability issues, since the perpendicular bisector may be parallel to the imaginary axis. Equation (2) does not have this problem. When β approaches zero, the last term on the right hand side of Eq. (2) will automatically approach zero. Equation (2) can be modified so that the transformed phasor field will gradually approach to the driving wave. To achieve this, Eq. (2) was modified to

$$\tilde{\mathrm{E}}_n = \tilde{\mathrm{E}}_{n-1} e^{j\omega\Delta t} + \Delta - j \cdot \frac{\left| \tilde{\mathrm{E}}_{n-1} e^{j\omega\Delta t} + \Delta \right|}{(\cos\alpha + \sin\alpha \cdot \cot\beta) M}, \tag{3}$$

where M is a damping factor and the magnitude is greater than 1. Figure 3 shows the simulation of transformations in using Eq. (3), with incoming wave $\mathrm{E}_n = 1 \cdot \sin(n \cdot 1^{\mathrm{o}}) + 0.01 \cdot \sin(n \cdot 100^{\mathrm{o}})$, and the second phasor field $\tilde{\mathrm{H}}_n$ being driven by $\mathrm{Re}\{\tilde{\mathrm{E}}_n e^{j\pi/8}\}$. The dash curve stands for $\tilde{\mathrm{E}}_n$, and the solid curve stands for H_n. As shown in Fig. 3, M leads to stability issue when it is a small number; however, when M is a large number, it will take longer time or more cycles to converge to a stable result.

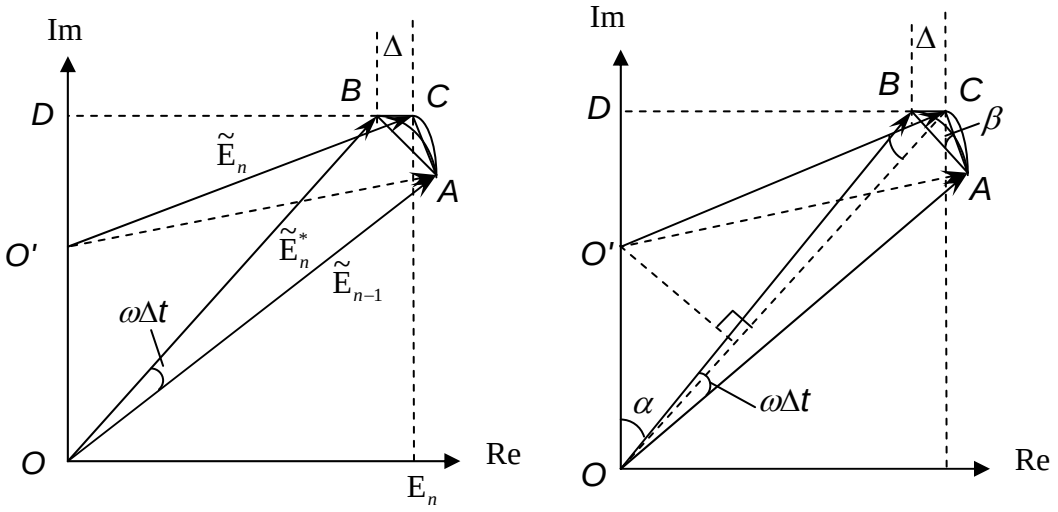

(a) (b)

Figure 2. Complex phasor representation of **E** fields at different time steps.

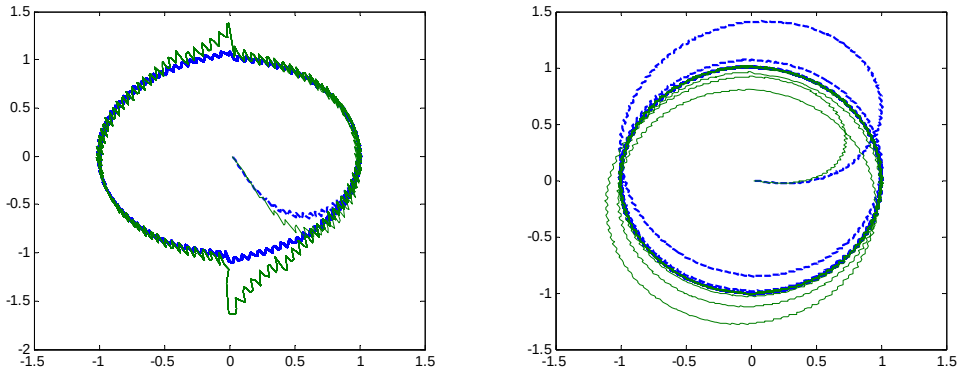

M = 20 M = 200

Figure 3. Phasor diagram based on Eq. (3).

CONCLUSIONS

Overall, the new technique can successfully treat the periodic boundary condition in the computational electrodynamics or any phase-dependent wave-propagation problem. The new method utilizes the given information (frequency of light source), instead of sampling a time period of signal to obtain the information as in the Fourier transform. Since the new transformation technique can instantly transform signal into phasor field, the method may have wide applications in dynamic system control and signal processing.